Research Square

Preprints are preliminary reports that have not undergone peer review.
They should not be considered conclusive, used to inform clinical practice,
or referenced by the media as validated information.

Phase-controlled Tribocorrosion Mechanisms in Heat-treated Electrodeposited Ni–mo–b Coatings

Svitlana Halaichak

svityliagolovey@gmail.com

G.V. Karpenko Physical-Mechanical Institute

Sergiy Korniy

G.V. Karpenko Physical-Mechanical Institute

Vadim Zakiev

National Aviation University

Vasyl Vynar

G.V. Karpenko Physical-Mechanical Institute

Maksym Danylchuk

G.V. Karpenko Physical-Mechanical Institute

Marian Chuchman

G.V. Karpenko Physical-Mechanical Institute

Roman Mardarevych

G.V. Karpenko Physical-Mechanical Institute

Yuriy Verbovytskyy

G.V. Karpenko Physical-Mechanical Institute

Research Article

Keywords: electrodeposited Ni–Mo–B coatings, tribocorrosion mechanism, heat treatment, Mo_2NiB_2, Ni3B, phase transformation

Posted Date: July 15th, 2026

DOI: https://doi.org/10.21203/rs.3.rs-9605682/v1

License: This work is licensed under a Creative Commons Attribution 4.0 International License.
Read Full License

Additional Declarations: No competing interests reported.

PHASE-CONTROLLED TRIBOCORROSION MECHANISMS IN HEAT-TREATED ELECTRODEPOSITED NI–MO–B COATINGS

Svitlana Halaichak[a], Sergiy Korniy[a], Vadim Zakiev[b], Vasyl Vynar[a], Maksym Danylchuk[a], Marian Chuchman[a], Roman Mardarevych[a], Yuriy Verbovytskyy[a]

[a]Karpenko Physico-Mechanical Institute of the National Academy of Sciences of Ukraine, L'viv, Ukraine

[b] National Aviation University, Kyiv, Ukraine

Corresponding author: svityliagolovey@gmail.com

Highlights

- Heat treatment at 950 °C induces the formation of Ni_3B and Mo_2NiB_2 phases in electrodeposited Ni‑Mo‑B coatings through diffusion-driven transformations.
- Increasing Mo content from 8 to 16 wt.% increases the Mo_2NiB_2 ternary boride fraction by a factor of 3.75.
- The evolution of phases greatly improves the micromechanical properties, achieving a hardness of up to 11.67 GPa and an elastic modulus of 292.5 GPa.
- The tribocorrosion mechanism shifts from oxidative‑adhesive wear to a stable, oxidation-dominated regime in 3% NaCl solution.
- High-Mo coatings exhibit 46% lower wear track width and improved friction stability under combined mechanical‑corrosive loading.

Abstract

This study establishes a direct relationship between heat-treatment-induced phase evolution and the tribocorrosion performance of electrodeposited Ni–Mo–B coatings. The coatings were deposited from a citrate electrolyte containing amorphous boron and then annealed at 950 °C in an inert atmosphere.

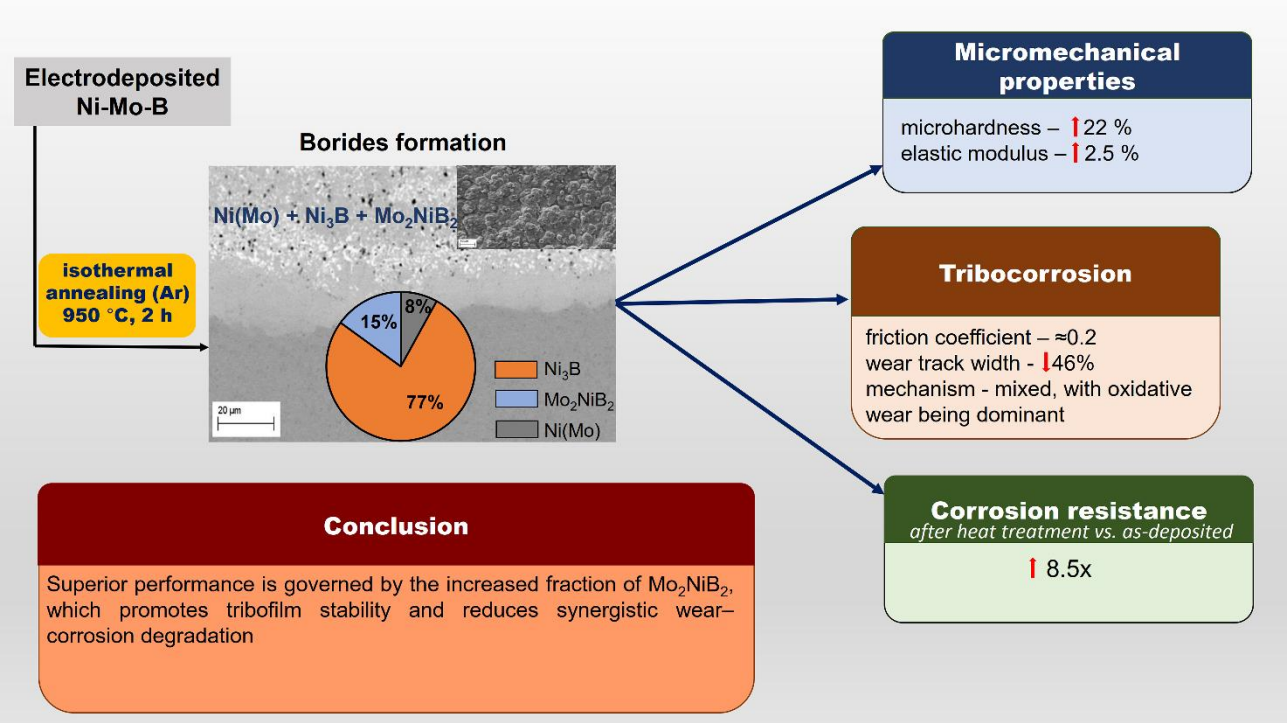
Heat treatment triggers a diffusion-driven transformation of amorphous boron, forming a composite microstructure consisting of a Ni(Mo) solid solution reinforced by Ni_3B and Mo_2NiB_2 borides. Increasing the Mo content from 8 to 16 wt.% increases the fraction of the Mo_2NiB_2 ternary boride by a factor of 3.75, which plays a key role in strengthening.

This phase evolution significantly enhances micromechanical properties, increasing hardness to 11.67 GPa and elastic modulus to 292.5 GPa. More importantly, it alters the dominant wear mechanism under tribocorrosion in a 3% NaCl solution: the system transitions from an unstable oxidative–adhesive regime to a stable oxidation-controlled mechanism with reduced friction fluctuations.

The coating with 16 wt.% Mo shows a 46% reduction in wear track width and stable friction behavior ($\mu \approx 0.2$), indicating superior resistance to corrosion–mechanical degradation. The results show that the fraction of the Mo_2NiB_2 phase governs the transition in wear mechanisms and the stability of tribocorrosion processes.

This work offers new insight into the design of boride-strengthened electrodeposited coatings, highlighting phase engineering as a key strategy to improve performance in aggressive environments.

Graphical abstract



Keywords: electrodeposited Ni–Mo–B coatings; tribocorrosion mechanism; heat treatment; Mo_2NiB_2; Ni_3B; phase transformation.

1. Introduction

Industrial equipment often faces combined mechanical tribological loads and aggressive environmental agents. This results in a decline in its functional properties, faster component wear, and early component failure, which, in turn, increases maintenance costs [1–4]. Therefore, a key area of research is the development of methods to enhance the wear and corrosion resistance of materials, especially to prevent tribocorrosive degradation [3, 5, 6]. One of the most common and effective ways to address this problem is to apply protective coatings. Nickel-based coatings are particularly promising because they can be alloyed with various elements, allowing the structure to be customized to meet specific functional requirements [7, 8]. Alloyed nickel coatings usually have a dense, fine-grained structure that prevents pores and cracks [5, 9], providing high corrosion resistance, resistance to high-temperature oxidation, and improved wear resistance in aggressive environments [4, 10]. In this context, Ni–Mo–B composite coatings show promise: molybdenum enhances corrosion resistance, while amorphous boron reduces internal stresses associated with high molybdenum content and improves wear resistance [5,11]. However, electrodeposited Ni–Mo–B coatings exhibit a non-uniform phase composition and limited hardness, potentially reducing their effectiveness under industrial operating conditions. In this regard, heat treatment is carried out to improve adhesion, reduce hydrogen embrittlement, and reduce residual stresses. Annealing is also accompanied by diffusion interaction of the components, with partial or complete dissolution of boron particles in the matrix and the formation of solid solutions and boride phases. Furthermore, the newly formed structural components occupy a larger volume in the matrix than the dispersed particles in the initial state. Therefore, it is an additional factor that increases the content of the strengthening phase in the coating, since electrochemical deposition cannot achieve the optimal volume fraction of the dispersed phase in the matrix (30–50%) to ensure high tribological characteristics.

From the standpoint of wear mechanisms, the formation of boride phases is critically important because they increase resistance to plastic deformation and reduce the severity of adhesive

and abrasive damage. Similar trends have been observed in thermodiffusion boriding of steels, where the formation of two-phase layers of FeB and Fe_2B results in a significant increase in hardness (17–21 GPa) and improved tribocorrosion resistance in aggressive environments. [12]. It has been shown that optimizing the boriding temperature determines the balance among hardness, brittleness, and stability of surface layers under loading conditions.

Boride coatings produced by thermodiffusion methods exhibit significantly lower mass loss and high resistance to delamination, even under the combined effects of friction, abrasive wear, and corrosion. This performance is attributed to their high hardness, chemical inertness, and ability to form stable tribofilms that reduce the real contact area and wear intensity. Similar behavior is observed in engineering systems operating in harsh environments, such as oil and gas equipment, where the synergistic effect of these factors significantly accelerates material degradation [13].

In addition to mechanical strengthening, tribochemical processes play an important role in tribocorrosion behavior. In particular, in systems containing molybdenum, oxide films form, which can act as solid lubricating layers with low shear resistance. It has been shown that in multicomponent Ni–Cr–Mo-based alloys, Mo-containing oxides form, thereby stabilizing the tribological contact and reducing the coefficient of friction [14]. Similarly, for Mo–Ni–Si systems, it has been established that the formation of passivation layers of the MoO_3–NiO–SiO_2 type reduces wear intensity and electrochemical degradation [15]. Such tribofilms play a key role in controlling degradation kinetics by limiting direct surface contact and hindering the penetration of aggressive media.

At the same time, despite significant progress in the study of boride materials, their application is associated with several limitations, including the need for high-temperature processing, difficulties in controlling coating thickness, and a tendency toward brittle failure. An alternative approach involves electrochemical deposition followed by heat treatment, enabling the controlled formation of strengthening phases without significant deterioration of adhesion or the coating's structural integrity.

Additionally, it has been established that increasing the boron content in coatings increases the fraction of the boride phase Ni_3B, accompanied by a significant enhancement in microhardness and wear resistance [16]. Ternary boride systems, such as Mo_2NiB_2, exhibit high mechanical and corrosion resistance [17–19], including increased hardness and resistance to aggressive environments [20–22]. However, the application of such materials is limited by technological difficulties in their synthesis and their restricted suitability as coatings.

Thus, despite existing advances, the relationship between thermally induced phase transformations, tribochemical film formation, and tribocorrosive wear mechanisms in Ni–Mo–B coatings remains insufficiently studied. In particular, the role of boride phases in controlling the coefficient of friction, wear rate, and electrochemical stability under combined loading conditions requires detailed analysis.

In this regard, the aim of this work is to determine the effect of heat treatment on the phase composition, microstructure, and tribocorrosion behavior of electrodeposited Ni–Mo–B coatings, as well as to elucidate the mechanisms of their tribocorrosion behavior. This will enable the development of scientifically grounded approaches to designing multifunctional coatings with enhanced wear and corrosion resistance for operation under severe combined loading conditions.

2. Materials and methods

2.1 Material

Low-alloy steel S355J2 samples measuring 30 mm × 40 mm × 5 mm were used in the experiments. The chemical composition of the steel is given in **Table 1**. Prior to electrodeposition, the steel was mechanically polished using silicon carbide (SiC) sandpaper with a grit size of up to

1200, after which it was ultrasonically cleaned in a cleaning solution to ensure the removal of any residual contaminants, treated with Vienna lime (CaO+MgO), rinsed with distilled water, and activated in a hydrochloric acid solution for 30 seconds, followed by rinsing with distilled water.

Table 1

Chemical composition [wt%] of S355J2 steel

C	Si	Mn	S	P	Cr	Ni
0.14	0.1	0.5	0.05	0.04	0.3	0.3

2.2 Electrodeposition

For the electrodeposition of Ni-Mo-B coatings, a suspension of amorphous boron (50 g/l) was used in an electrolyte containing 0.2 M $NiCl_2$, 0.3 M $Na_3C_6H_5O_7$, saturated $SrMoO_4$, and pH 9.0 (ammonia) [5]. The electrolyte was prepared from analytical-grade reagents and distilled water; boron was of technical grade. The chemical composition of the initial boron used to prepare its suspension, wt. %: B – 93.81; Mg – 0.43; O – 4.75; Fe – 0.05; Si – 0.08; other impurities – 0.10. The reagents were purchased from a private company «System Optimum».

Electrodeposition of the coatings was performed at 60±1 °C, using current densities of 2.5 and 5.0 A/dm^2, with a stirring speed of 300 rpm for 1 hour. A nickel plate measuring 40 × 50 × 2 mm served as the anode. The distance between the electrodes was set at 40 mm. A thermocouple monitored the bath temperature, and continuous mechanical stirring was maintained to ensure electrolyte homogeneity. The electrolyte volume was 500 ml.

2.3 Heat treatment

Heat treatment (isothermal annealing) of the coated samples was performed in a SSOL-1.1.6/12 shaft-type electric furnace at 950 °C for 2 hours in an inert (Ar) atmosphere. Temperature uniformity within the crucible's working volume was ±10 °C, and the heating rate was 9 °C/min. To prevent surface oxidation, the samples were placed in a sealed cylindrical stainless steel (310S) container, through which argon was flowed at 70–75 l/h. The purified gas was supplied to the container using a PD-2012 unit (Sirkal Instruments).

2.4. Coating Characteristics

2.4.1 Morphology, chemical composition, and structure of the coatings

The surface morphology and elemental composition of the Ni-Mo-B coatings were analyzed using a Zeiss EVO-40XVP scanning electron microscope fitted with an Oxford UltimMax 65 energy-dispersive spectrometer (EDS) and AZtecLive spectrum-processing software. The reported chemical composition is the average of three measurements taken at different locations on the coating surface.

The structure and phase composition of the coatings were analyzed using an AERIS Research X-ray diffractometer with Mn-filtered Cu radiation at U = 30 kV, I = 15 mA, a 2θ step of 0.025°, and a counting time of 1.5 seconds. The Rietveld method was used to refine the profile and structural parameters by comparing the calculated diffractogram with the experimental data.

2.4.2. Micromechanical properties

The micromechanical properties were determined using the sclerometry and dynamic nanoindentation methods on the 'Micron-Gamma' multifunctional instrument [23]. The microhardness and elasticity of the materials were determined using the Oliver-Farr method [24], as specified in ISO/FDIS 14577-1: 2002 [25]. Indenter load: 50 g; range of measured displacements: 0.01–200 μm; indenter loading rate: 5 g/s; table displacement range: 25×25 mm.

2.4.3. Corrosion resistance

The corrosion resistance of the coatings was tested in a 3% NaCl solution under argon bubbling to remove oxygen. Electrochemical evaluations of the coatings were performed in a potentiostatic mode using the Mtech SPG-500 fast potentiostat-galvanostat. The reference electrode

used was a silver chloride type EVL-1M1, and the auxiliary electrode was platinum. The potential scan rate was set to 1 mV/s. The reduction and oxidation potentials were recorded relative to an Ag|AgCl|KCl (saturated) electrode and standardized against a standard hydrogen electrode. The results were averaged after testing three samples.

2.4.4. Tribocorrosion properties

Tribocorrosion tests on coated plate specimens were conducted using the ‘‘plane–ball’’ method on a friction test rig with reciprocating movement of the contact surfaces and a friction half-cycle of 16 mm [26]. The load on the indenter (Al2O3, d = 9 mm) was 10 N; the working medium was a 3% NaCl solution.

3. Results and discussion

3.1. Structural and phase composition and morphology of the coatings

The results of the chemical analysis showed that the electrodeposited coatings produced at current densities of 2.5 and 5.0 A/dm^2 contain nickel, molybdenum, and boron, with wt %: 81.11 Ni; 16.00 Mo; 2.89 B, and 88.61 Ni; 8.00 Mo; 3.39 B, respectively. No other elements were detected. The XRD analysis indicated that the coatings consist of a solid solution of molybdenum in nickel, nickel boride Ni_3B, and the complex boride of nickel and molybdenum Mo_2NiB_2 (**Fig. 1**). The boride phase content is 71% and 92%, at Mo contents of 8 and 16 wt%, respectively (**Table 2**).

a **b**

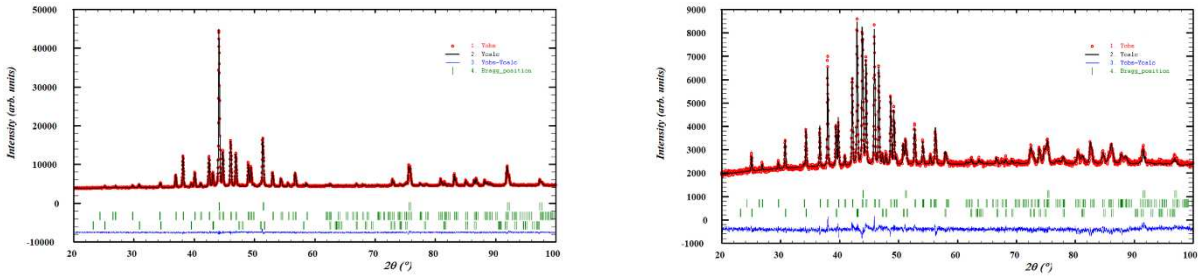


Fig. 1. X-ray diffraction patterns of Ni-Mo-B coatings with Mo content in wt%: **a**) 8; **b**) 16; (|- Ni(Mo); | |- Ni_3B; | | |- Mo_2NiB_2).

Table 2.

Results of the phase analysis of the coatings

Mo content, wt%	Phase content (%)		
	Ni (Mo)	Ni_3B	Mo_2NiB_2
8	29	67	4
16	8	77	15

Cross-sectional views of the coatings reveal a matrix-filled composite structure with a clearly defined transition diffusion zone at the interface with the substrate (**Fig. 2a, b**). In the central regions of the boride grains, unreacted impurities of technical boron (black inclusions) are present–namely, magnesium borides and oxides, whose presence is influenced by the method of boron production and its refining. As a result of the diffusion-driven dissolution of boron particles in the Ni–Mo metallic matrix under the specified heat treatment conditions, the formation of new boride structures is observed. No cracks or pores were observed in the SEM images of the coatings (**Fig. 2a$^/$, b$^/$**). The surface features large, irregularly oval agglomerates, with decreasing size as the molybdenum content increases.

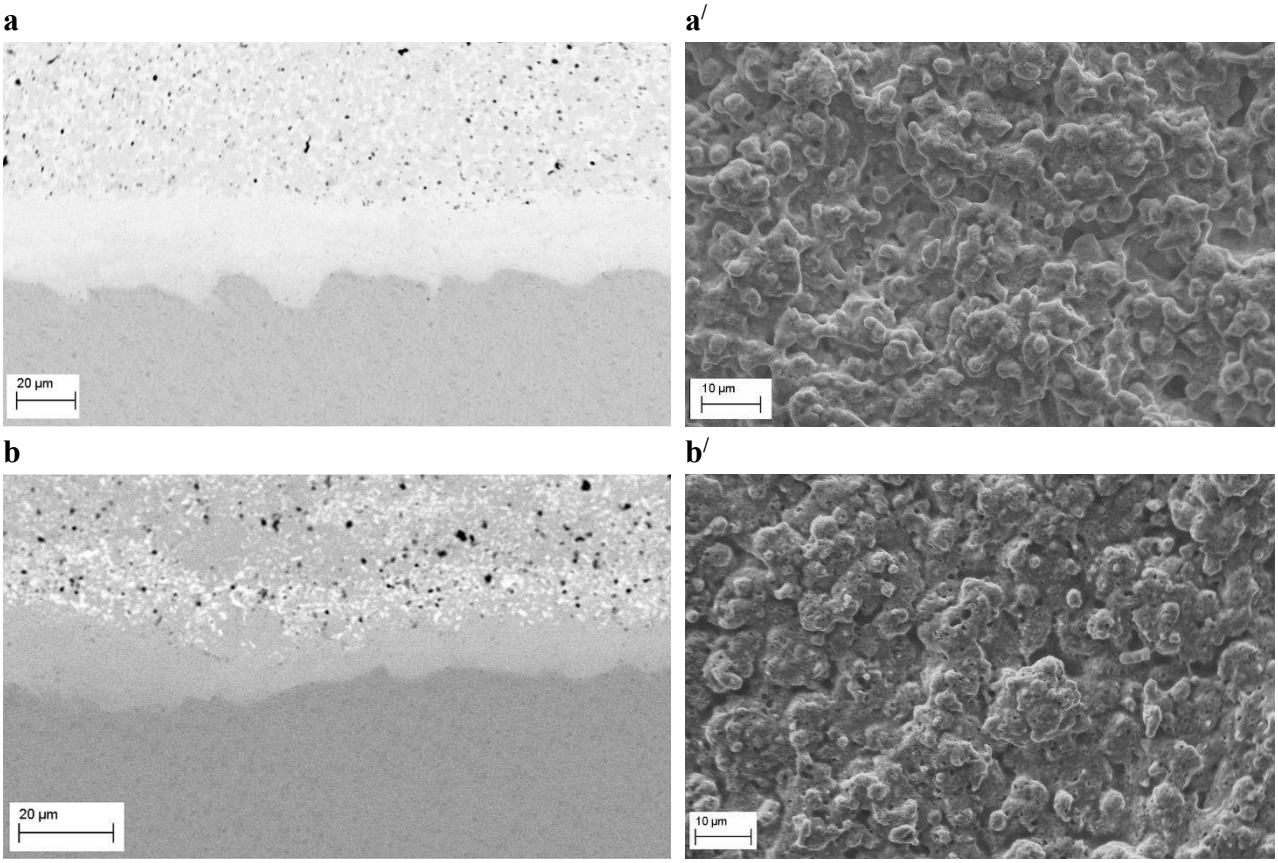


Fig. 2. Microstructure and corresponding SEM images (/) of the surface of Ni-Mo-B coatings with Mo contents in wt%: **a**) 8; **b**) 16.

From a wear-mechanism perspective, this refinement is significant because finer, more uniformly distributed hard phases reduce stress localization and delay crack initiation during sliding contact.

3.*2. Corrosion resistance of coatings*

Anodic polarization of the coatings in a 3% NaCl solution to approximately 0.12 V leads to their active dissolution, with the dissolution rate being about 4–6 times higher on coatings with Mo content of 8 wt%. (Fig. 3). As the potential shifts further toward the anodic side, a passivation plateau appears due to the formation of oxide-hydroxide compounds. This passive layer effectively prevents the diffusion of aggressive chloride ions into the coating's matrix. The corrosion potentials and current densities of the coatings do not differ significantly, most likely due to the formation of passive films of similar composition and a comparable coatings morphology. However, it is notable that Ni-Mo-B coatings exhibit ~30% greater corrosion resistance than hard electroplated chromium coatings produced under direct current [27]. For the initial (unheat-treated) Ni-Mo-B coatings with 8 and 16 wt% Mo content, the corrosion resistance is approximately ~18.6 and ~8.5 times lower, respectively [5], than that of the heat-treated coatings.

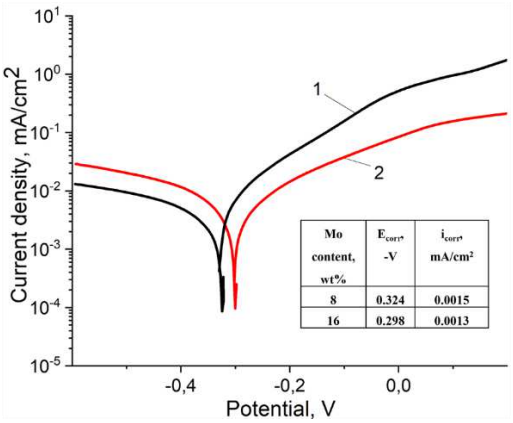


Fig. 3. Polarization curves in 3% NaCl solution for Ni-Mo-B coatings with different Mo contents in wt%: **1** – 8; **2** – 16.

From a tribocorrosion perspective, this improvement is critical because electrochemical stability directly affects the ability to maintain protective tribofilms under sliding contact.

3.3 Micromechanical properties

The results of dynamic indentation (Table 3) show that heat treatment of Ni-Mo-B coatings improves their resistance to localized contact loading compared to the as-received state. Increasing the molybdenum content in the coatings decreases the indenter penetration depth both at maximum load (h_1) and after unloading (h_2). These changes are associated with increased microhardness ($H_{v0.05}$) and elastic modulus (E), indicating greater resistance to local deformation. The increase in the microhardness and stiffness of the coatings is due to the higher content of the Mo_2NiB_2 boride phase (with a hardness of ~20 GPa [16]) as the molybdenum content increases from 8 to 16 wt%.

Table 3.

Results of dynamic indentation testing of the coatings

Mo content, wt%	h_1	h_2	$H_{v0.05}$, GPa	E, GPa	$W_{plastic}$	$W_{elastic}$	ε
	μm				μJ		
8	1.461	1.286	9.555	285.3	28.49	10.9	0.62
16	1.317	1.122	11.670	292.5	23.96	10.1	0.63

The mechanical property results show a ~16% decrease in the specific plastic work of deformation ($W_{plastic}$) and a slight decrease in the specific elastic work ($W_{elastic}$) with increasing molybdenum content, indicating that the coating is mainly strengthened by dispersion.

The increase in the elastic strain index (ε) from 0.62 to 0.63 indicates improved elastic recovery of Ni–Mo–B coatings, reflecting increased resistance to plastic deformation due to dispersion strengthening by Ni_3B and Mo_2NiB_2 boride structures in the Ni–Mo matrix. From a wear perspective, this implies reduced plastic grooving severity, improved resistance to subsurface deformation, and a delayed transition from mild to severe wear regimes.

3.4 Sclerometric tests

The results of sclerometric studies (**Fig. 4**) show that for the coating with 8 wt % Mo, a sharp decrease in the resistance force to displacement is observed along a scan track length of ~630 μm.

The indenter's movement involves elastic-plastic interaction and causes local damage, specifically microcutting. Wear products are present on the surface. This conclusion is supported by the topography of the friction surface (**Fig. 5a**) and indicates the coating's high cohesive strength and its adhesion to the substrate. For the coating with 16 wt % Mo, the opposite pattern is observed: at

the beginning of the scan track, the resistance to displacement is lower compared to the previous coating, and then it gradually increases. This behavior is explained by the accumulation of damage in the form of cracks on the friction track (**Fig. 5b**), caused by the greater brittleness of the surface layers and their destruction due to the action of high local stresses.

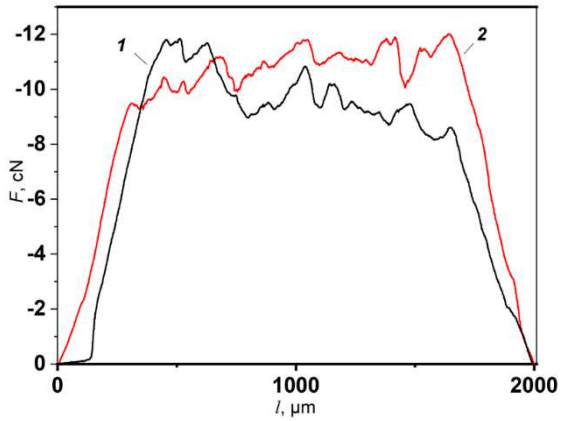


Fig. 4. Variation in the resistance force during indenter movement across the surface of Ni-Mo-B composite electrochemical coatings with Mo contents in wt%: **1** – 8; **2** – 16

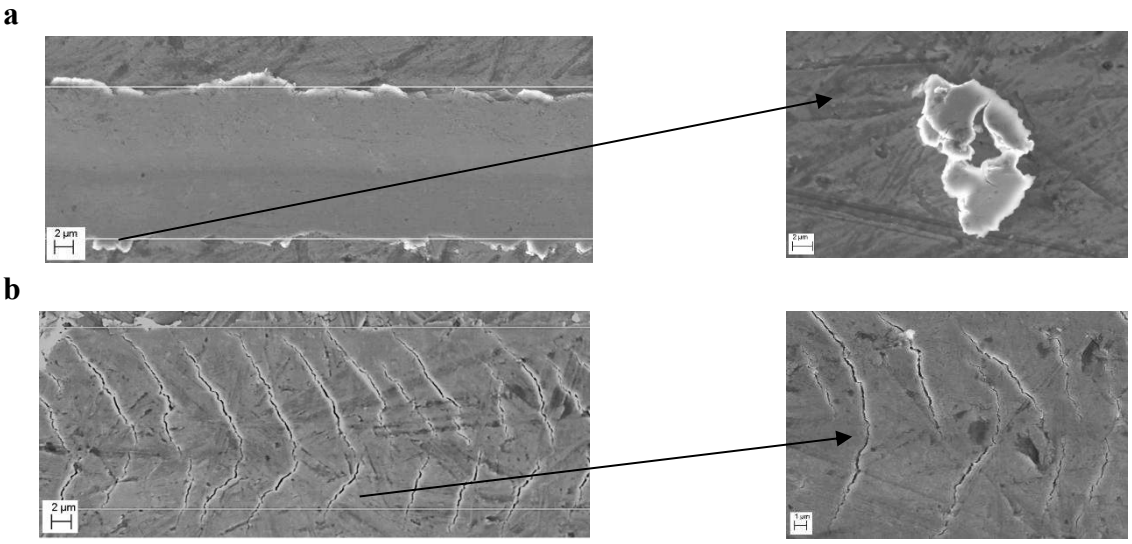


Fig. 5. Surface topography of friction tracks on Ni-Mo-B composite electrochemical coatings with Mo contents of **a**) 8; **b**) 16wt%.

Therefore, the sclerometric data and surface topography confirm that increasing the Mo content from 8 to 16 wt% transforms the mechanism from pure micro-cutting to a mixed mechanism involving micro-cutting, adhesive bonding, and elements of fracture formation.

3.5 Tribocorrosion properties of the coatings

Changes in coating composition after heat treatment alter their microstructural and phase states, significantly impacting their tribocorrosion properties. Due to the enhanced micromechanical properties of the running-in zone, wear in a chloride-containing environment is nearly negligible for both molybdenum concentrations (**Fig. 6a, b**). At the start of the tests, the average coefficient of friction is about 0.2 for both coatings.

For the 8 wt% Mo coating, the friction process is characterized by a gradual increase in the coefficient of friction over time, linked to damage accumulation in the surface layers due to adhesive interactions between the contacting surfaces. This is indicated by local fluctuations in the coefficient of friction during a single pass of the indenter: between 1002 and 1008 seconds, fluctuations reach ±0.026 of the average value (**Fig. 6c**). In this case, an oxidative–adhesive friction mechanism with elements of microdeformation dominates.

The 16 wt% Mo coating shows higher microhardness and improved micromechanical properties, leading to more stable friction behavior with minimal changes in the coefficient of friction throughout the test and smaller local fluctuations (**Fig. 6b, c**). Here, a mixed wear mechanism prevails, with the oxidative process being dominant.

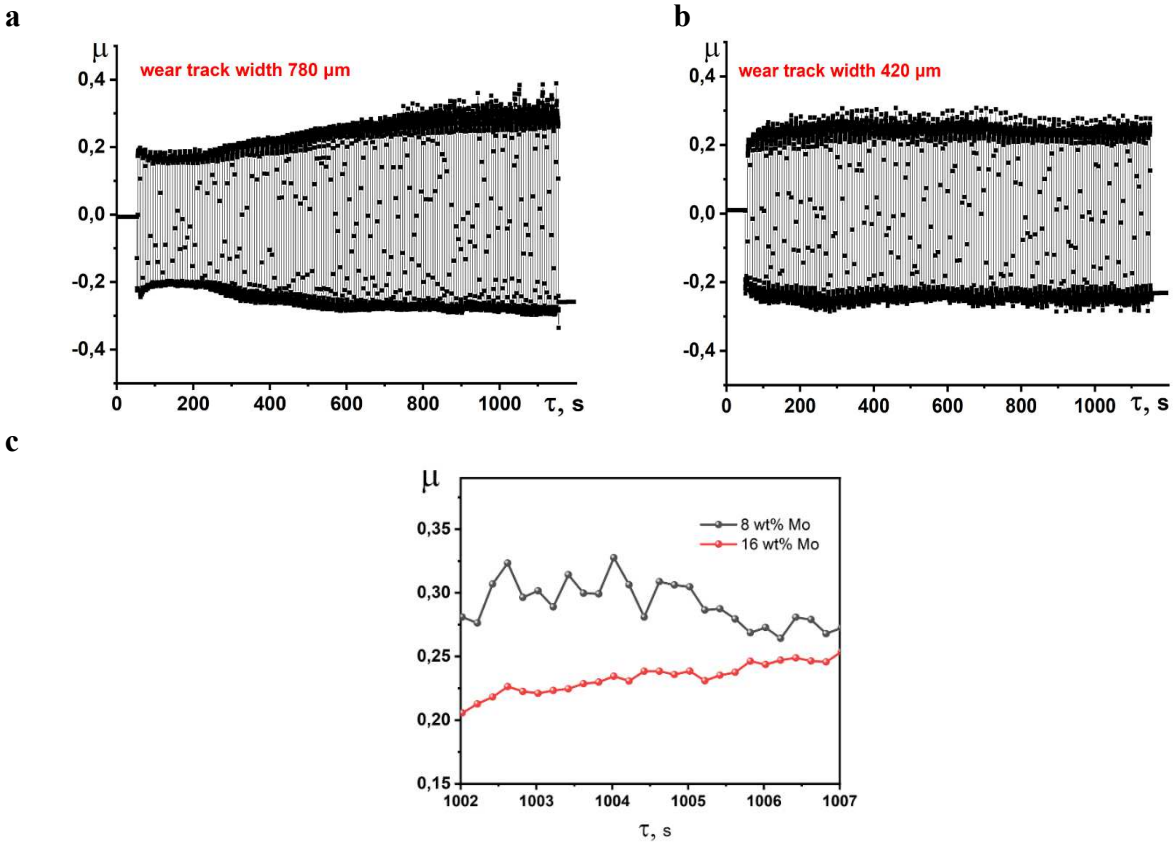


Fig. 6. Overall variation in the coefficient of friction of Ni-Mo-B coatings with Mo content in wt%: **a**) 8; **b**) 16, and **c**) local variation in the coefficient of friction over a single pass.

Changes in the wear mechanisms are confirmed by electrochemical studies and metallographic analysis of surfaces after tribocorrosion testing of the coatings. It was found that the electrode potential clearly correlates with changes in the coefficient of friction: as the coefficient of friction increases, the tribopotential shifts toward more negative values, indicating surface activation and the intensification of tribocorrosion processes (**Fig. 7**). At the initial stage, the surface activation of the heat-treated composite layer with 8 wt% Mo is approximately 10 mV higher than that of the coating with 16 wt% Mo, and the potential remains nearly unchanged as the number of cycles increases. Consequently, the 8 wt% Mo coating, with fewer strengthening structural-phase components, undergoes damage in the form of micro-galling and micro-scoring (**Fig. 8a**). In the case of the 16 wt% Mo coating, only traces of interaction between the coating and the corundum counterpart are observed, without significant damage (**Fig. 8b**). This leads to an increase in the coefficient of friction and a shift of the tribopotential toward more negative values, reproducing the trend observed for the coefficient of friction.

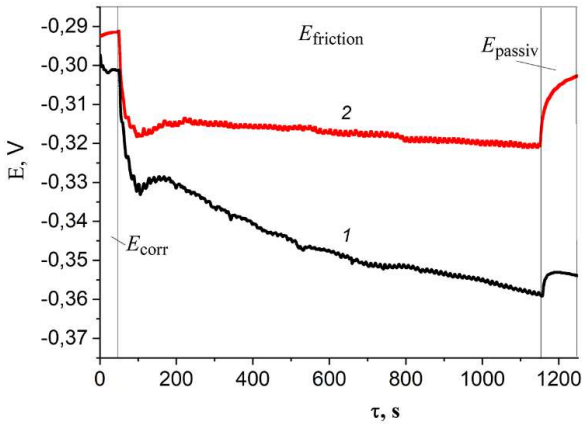


Fig. 7. Change in electrode potential during tribocorrosion testing of Ni-Mo-B coatings with Mo content in wt%: **1** – 8; **2** – 16.

a **b**

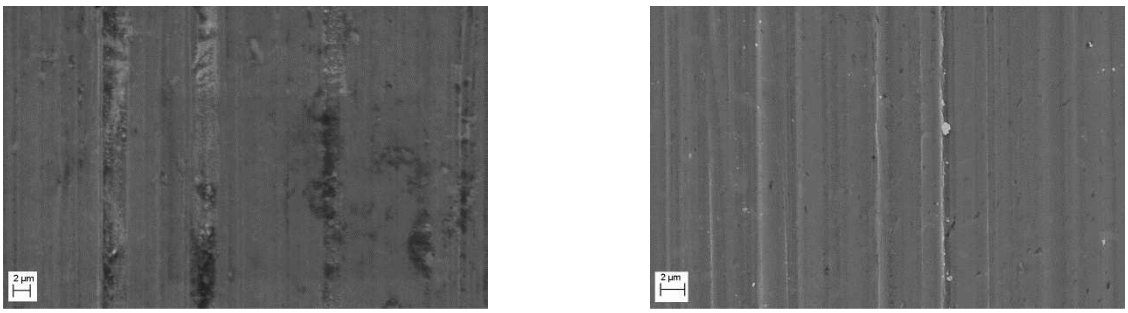


Fig. 8. Topography after tribocorrosion testing of Ni-Mo-B electrochemical coatings with Mo content in wt%: **a**) 8; **b**) 16.

The width of the wear track at the higher molybdenum concentration is approximately 420 µm, whereas at the lower concentration it is around 780 µm. This indicates that the coating with 16 wt% molybdenum exhibits higher wear resistance under corrosion–mechanical wear conditions than the coating with 8 wt%, and can therefore be used to enhance tribocorrosion resistance.

Consequently, increasing the molybdenum content to 16 wt% in Ni–Mo–B coatings after heat treatment ensures the formation of a more strengthened structural–phase state, which contributes to the stabilization of tribocorrosion interaction, a reduction in the coefficient of friction, a decrease in the width of the wear track, and an increase in resistance to corrosion–mechanical damage. This is attributed to the higher content of strengthening phases, in particular the Mo_2NiB_2 ternary boride, whose fraction is 3.75 times higher. As reported in the literature [18], this leads to improved wear resistance and enhanced tribocorrosion properties of the materials.

4. Conclusions

Heat treatment at 950 °C induces diffusion-driven formation of Ni_3B and Mo_2NiB_2 phases in Ni–Mo–B coatings, and their fraction increases with Mo content. The resulting microstructure strongly governs tribocorrosion behavior..

Key findings from a wear-mechanism perspective:

• Boride dispersion strengthening increases hardness (up to 11.67 GPa) and elastic modulus (up to 292.5 GPa), reducing plastic grooving and stabilizing contact deformation.

• Corrosion resistance improves significantly due to the formation of a stable passive film, enhancing tribofilm durability under sliding conditions.

• Increasing Mo content shifts the wear mechanism from oxidative–adhesive to mixed wear with dominant oxidative stabilization, reducing friction instability.

• Tribocorrosion resistance improves substantially at 16 wt.% Mo, as evidenced by stable friction (~0.2), reduced wear track width (−46%), and lower tribopotential fluctuations.

• Superior performance is governed by the increased fraction of Mo_2NiB_2, which promotes tribofilm stability and reduces synergistic wear–corrosion degradation.

Overall, Ni–Mo–B coatings with 16 wt.% Mo demonstrate the most stable tribocorrosion response under chloride-containing sliding conditions, making them promising candidates for protective applications in oil, gas, and chemical engineering systems subjected to severe combined wear–corrosion loading.

Funding Information

This work was supported by the National Academy of Sciences of Ukraine (project number 0224U033049).

Author contributions

Svitlana Halaichak: Conceptualization, Methodology, Investigation, Writing -original draft. **Sergiy Korniy**: Project administration, Writing - review & editing. **Vadim Zakiev**: Investigation, Writing – review and editing. **Vasyl Vynar**: Software, Investigation. **Maksym Danylchuk**: Methodology, Visualization, Investigation. **Marian Chuchman**: Methodology, Writing - review & editing. **Roman Mardarevych:** Methodology, Conceptualization, Writing - review & editing. **Yuriy Verbovytskyy**: Methodology, Investigation. All authors have read and agreed to the published version of the manuscript.

Ethics declarations

Ethics approval and consent to participate

This study did not involve human participants, human data, human tissue, or animals; therefore, ethical approval and consent to participate were not required.

Conflict of Interest

The authors declare that they have no known competing financial interests or personal relationships that could have influenced the work reported in this paper.

Data availability statement

During this investigation, all data produced or analyzed are contained within the published manuscript. The datasets generated during and/or analyzed during the current study are available from the corresponding author on reasonable request.

References

1. Sreekumar R., Nair A. (2022). Recent trends and developments in two-dimensional materials based electrodeposited nickel nanocomposite coatings. FlatChem 36:100434. https://doi.org/10.1016/j.flatc.2022.100434.
2. Zhao X., Hou Y., Ren Z., Liu M. (2025). Progress of electrodeposition of nickel-based anticorrosive wear-resistant coatings in deep eutectic solvents. J Electrochem Soc 172:102505. https://doi.org/10.1149/1945-7111/ae0eb4.
3. Zhang L., Shang C., Wang F., Zheng T., Nie C., Qiao Y. et al. (2025). The wear behavior and corrosion resistance properties of Ni-based composite coatings modified with CeO_2 and MoS_2 nanoparticles. Colloids Surf A: Physicochem Eng Asp 719:137017. https://doi.org/10.1016/j.colsurfa.2025.137017.
4. Chen J., Lu W., Dai P., Wen X., Wang Z., Fan H. et al. (2025). Evolution in wear, corrosion, and tribocorrosion behavior of Ni-based alloys induced by Mn addition. Wear 570:205895. https://doi.org/10.1016/j.wear.2025.205895.

5. Halaichak S., Korniy S., Zakiev V., Vynar V., Danylchuk M., Chuchman M., Mardarevych R. (2026). Corrosion resistance, wear resistance, and tribocorrosion of Ni-Mo-B electrodeposited coatings. Mat Sci 61:645-55. https://doi.org/10.15407/pcmm2025.05.012.
6. Zellele D., Zhamanbayeva G., Kemelzhanova A., Atchibayev R., Kurmangaliyeva V. (2025). Microstructure, tribological and corrosion resistance properties of Ni composite coatings prepared via electrodeposition. SGEM 6:57-63. https://doi.org/10.5593/sgem2025/6.1/s23.08.
7. Guler O., Çelebi M., Karabacak A. (2026). Latest Developments for Ni-Based Wear Protective Surfaces: Coating Compositions and Methods. In: Altalhi I.T., M.A. Mazumber, editors. Nanostructured hard materials: industrial applications, Beverly: John Wiley & Sons, p.39-111. https://doi.org/10.1002/9781394314171.ch2.
8. Sun H., Shi P., Yi G., Feng X., Shan Y., Wang J. et al. (2026). Tribological performance of metal matrix composites for high-temperature applications: a review with emphasis on nickel-based composite coatings. Compos Des Manuf wqag010. https://doi.org/10.1093/cdm/wqag010.
9. Trabelsi D., Nasri F., Kharrat M., Pereira A., Cardoso C., Eyraud M. et all. (2025). Electrodeposited composite coatings based on Ni matrix filled with solid lubricants: Impact of processing parameters on tribological properties and scratch resistance J Comp Sci 9:246. https://doi.org/10.3390/jcs9050246.
10. Vinay R., Vinod B., Baburao P., Amosedinakaran S., Ponnuru S. Assessment and electrodeposition of high-quality Ni-based thin films: enhancing high-temperature composites for robotic devices. ICCPCT 1256-61. https://doi.org/10.1109/ICCPCT65132.2025.11176671
11. Halaichak S., Vynar V., Khoma M., Mardarevych R., Ivashkiv V., Korniy S. (2023). Increasing corrosion resistance of Ni-Mo composite electrodeposited coatings: doping with boron. Mat Lett 353:135268. https://doi.org/10.1016/j.matlet.2023.135268.
12. Alkan S., Günen A., Gülen M., Gök M. (2024). Effect of boriding on tribocorrosion behavior of HSLA offshore mooring chain steel. Surf Coat Techn 476: 130276.https://doi.org/10.1016/j.surfcoat.2023.130276.
13. Medvedovski E., Jiang J., Robertson M. (2016). Iron boride-based thermal diffusion coatings for tribo-corrosion oil production applications. Ceram Internat 42 (2): 3190-3211.https://doi.org/10.1016/j.ceramint.2015.10.109.
14. Huang L., Wang Z., Chen M., Wang F. (2025). Effect of Nb/Mo addition on the tribocorrosion behavior of Ni20Cr-based alloy in 3.5 wt% NaCl solution. Trib Internat 216: 111554.https://doi.org/10.1016/j.triboint.2025.111554.
15. Chen H., Li R., Liu L., Zhang Z., Zhao X. (2024). Structural, mechanical and tribocorrosion behaviors of Mo-Ni-Si alloys. Trib Internat 196: 109723.https://doi.org/10.1016/j.triboint.2024.109723.
16. Diabb J., Juarez-Hernandez A., Colas R,. Castillo A., Garcia-Sanchez E, Hernandez-Rodriguez M. (2009). Boron influence on wear resistance in nickel-based alloys. Wear 267: 550-555. https://doi.org/10.1016/j.wear.2008.12.046.
17. Takagi K. (2006). Development and application of high strength ternary boride base cermets. J Solid State Chem 179:2809–18. https://doi.org/10.1016/j.jssc.2006.01.023.
18. Shangguan D., Lang H., Tang S., Wang X., Jiang X., Wang G., Wang J. (2025). Preparation and mechanical properties of high-entropy boride-based cermet based on ternary boride. J Mat Sci 60:11296-310. https://doi.org/10.1007/s10853-025-11036-9.
19. Yu M., Zhang X., Li W., Ai T., Dong H., Yang Z. (2025). Study of Mo_3NiB_3 and Mo_2NiB_2 cermets by first-principles calculation and experiment. Next Mater 7: 100324. https://doi.org/10.1016/j.nxmate.2024.100324.
20. Yuan B., Zhang G., Kan Y., Wang P. (2010). Reactive synthesis and mechanical properties of Mo_2NiB_2 based hard alloy. Int J Refract Met Hard Mater 8:291-96. https://doi.org/10.1016/j.ijrmhm.2009.11.002.
21. Zhang L., Gao Y., Huang Z., Ma H., Liu Y., Jie W., Zhou L. (2023). Effect of Ni content on the corrosion behavior of Mo_2NiB_2–Ni cermet in H_2SO_4 solution. Ceram Int 49:36289-298. https://doi.org/10.1016/j.ceramint.2023.08.311.
22. Yang Z., Liang H., Zhang H., Zhang L., Yu F., Li W., Zhang X. (2024). A novel wear-resistant and corrosion-resistant Mo_2NiB_2–Ni cermet coating prepared using fast hot pressing sintering. Mater Chem Phys 318: 129242. https://doi.org/10.1016/j.matchemphys.2024.129242.
23. Storchak M., Zakiev I., Traris L.(2018). Mechanical properties of subsurface layers in the machining of the titanium alloy Ti10V2Fe3Al. J Mech Sci Technol 32:315–22. https://doi.org/10.1007/s12206-017-1231-9.
24. Oliver W., Pharr G. (1992). An improved technique for determining hardness and elastic modulus using load and displacement sensing indentation experiments. J Mater Res 7:1564–80. https://doi.org/10.1557/JMR.1992.1564.

25. ISO/FDIS 14577-1: 2015 Metallic materials – Instrumented indentation test for hardness and materials parameters Part 1: Test method, Geneva. ISO Central Secretariat 2015. https://www.iso.org/standard/56626.html.
26. Vynar V., Dovhunyk V., Student M. (2011). Methodical specific features of tribocorrosion investigations. Mater Sci 46:633-39. https://doi.org/10.1007/s11003-011-9334-4.
27. Beyragh M., Asl S., Norouzi S. (2010). A comparative research on corrosion behavior of a standard, crack-free and duplex hard chromium coatings. Surf coat technol 205:2605-10. https://doi.org/10.1016/j.surfcoat.2010.10.009.